

RESEARCH

Open Access



Exploring the efficacy of *Pongamia pinnata*-induced silver nanoflowers for efficient adsorptive degradation of malachite green dye

Sneha Nayak^{1*}, Louella Concepta Goveas¹ and Shyama Prasad Sajankila¹

Abstract

In this study, silver nanoflowers were synthesized due to catalytic reduction of silver ions by phytochemicals of *Pongamia pinnata* seed cake extract (PSCAgNPs) in 24 h and subsequently used for removal of malachite green (MLG) dye. PSCAgNPs were characterized by UV-Visible spectrophotometry, scanning electron microscopy (SEM), energy-dispersive X ray spectroscopy (EDAX), Fourier Transformed Infrared Spectroscopy (FT-IR), X-Ray Diffraction (XRD) and BET analysis. The synthesized PSCAgNPs were floral in appearance, of size 18.82—23.70 nm with SPR at 430 nm and crystalline in nature. PSCAgNPs adsorbed $90.01 \pm 0.17\%$ of 50 mg/L MLG post one factor at a time analysis. Adsorption followed pseudo-second-order kinetics ($k_1 = 2.5E-03$ g/mg.h), was observed as unilayer chemisorption as the equilibrium data best fitted Langmuir isotherm (Langmuir coefficient = 0.1724 L/mg, $R^2 = 0.9945$). Upon interaction of MLG by PSCAgNPs, hydroxylation of MLG leads to formation of MLG carbinol in the first stage of adsorptive degradation, as evident from LCMS chromatograms.

Keywords Green synthesis, Dye, Remediation, Adsorption, Degradation

*Correspondence:

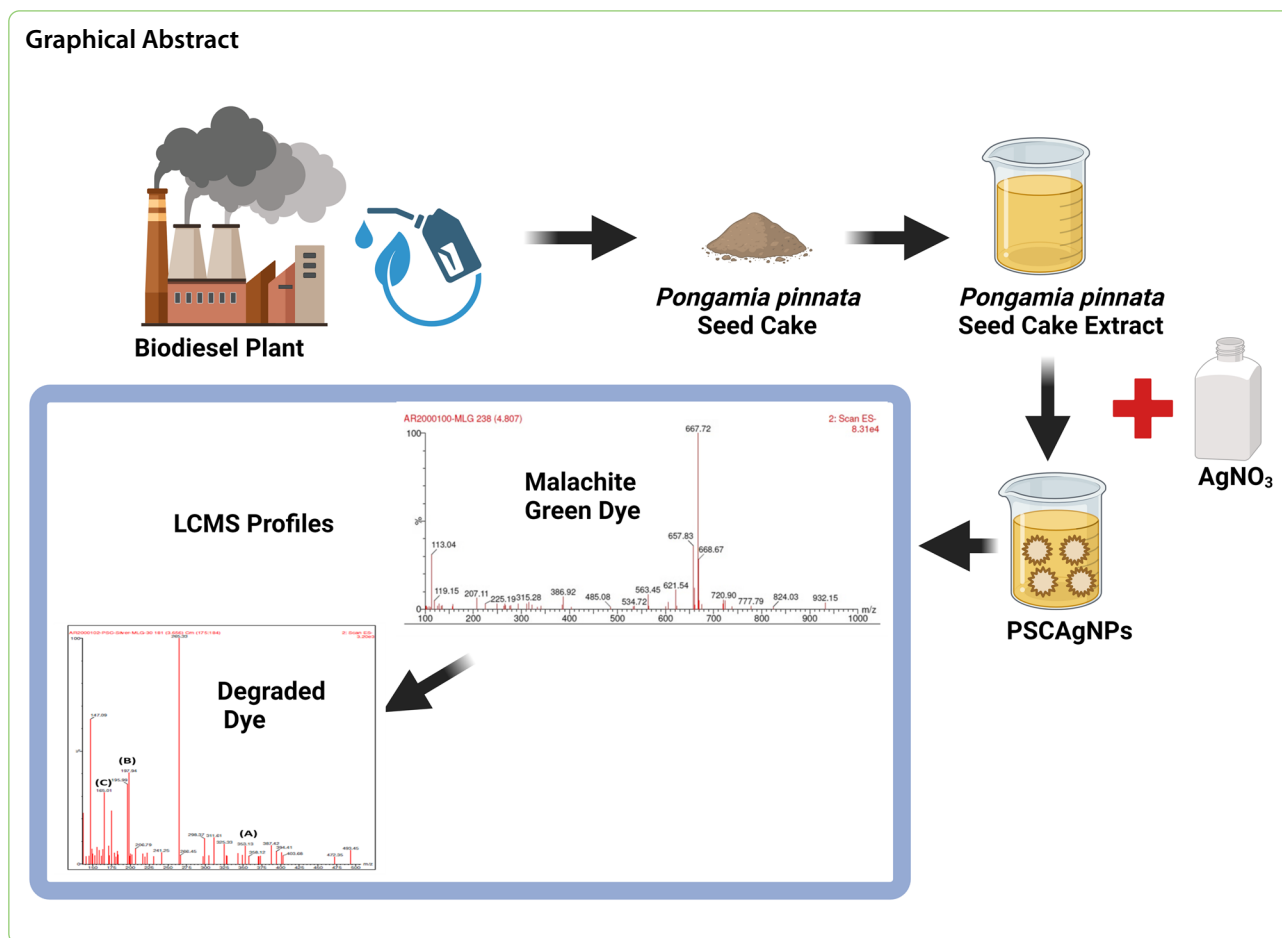
Sneha Nayak

snehanayak@nitte.edu.in

Full list of author information is available at the end of the article



© The Author(s) 2024. **Open Access** This article is licensed under a Creative Commons Attribution-NonCommercial-NoDerivatives 4.0 International License, which permits any non-commercial use, sharing, distribution and reproduction in any medium or format, as long as you give appropriate credit to the original author(s) and the source, provide a link to the Creative Commons licence, and indicate if you modified the licensed material. You do not have permission under this licence to share adapted material derived from this article or parts of it. The images or other third party material in this article are included in the article's Creative Commons licence, unless indicated otherwise in a credit line to the material. If material is not included in the article's Creative Commons licence and your intended use is not permitted by statutory regulation or exceeds the permitted use, you will need to obtain permission directly from the copyright holder. To view a copy of this licence, visit <http://creativecommons.org/licenses/by-nc-nd/4.0/>.



Introduction

Rapid industrialization to satisfy human needs has led to the production of harmful textile effluents which has detrimental effects on human health and environment if not treated before discharge [3]. Since it is inevitable that harmful chemicals like dye will be used in industry, it is necessary to take appropriate corrective action before releasing it into water bodies [5]. Dyes are intricate organic molecules that are frequently used to add colour to a variety of materials, including paper, fur, cosmetics, pharmaceuticals, textiles, leather, plastic and more [52, 59]. Chromophore, is the complex part of the dye which is highly resistant to degradation [49]. Despite having the ability to render their effluent safe before disposal, textile businesses fail to do so, introducing phthalates, heavy metals, and dyes to water bodies [42]. More than a million different varieties of dyes are widely utilised on a commercial scale, and between 7 and 10 million tonnes of dyes are manufactured each year [34]. For instance, approximately 2.8 million tons of deadly dyes reach the effluent stream post the dyeing process which needs to be remediated [9, 30]. Malachite green (MG) dye, a widely

explored dye in textile and aquaculture industry poses severe threat to health and environment due to its nature of persistence. mutagenic and carcinogenic nature of this dye necessitates effective removal strategies which are sustainable and cost effective [53].

For the eradication of dye containing effluent numerous techniques have been explored which includes coagulation-flocculation [20], biodegradation [22], Photocatalytic removal [16], electrochemical oxidation integrated with chemical oxidation [29], ion exchange [24], advanced oxidation process [43], membrane technology [1], ozonation [58], electrocoagulation [57], and adsorption [17, 36]. Adsorption is a technique which is widely accepted for dye remediation due to its low cost and ease in scaling up without much practical difficulties [23, 55]. Even though many researchers have focussed on microbial assisted degradation of dyes in the recent past requirement of laborious culture maintenance makes it an uneconomical option for real time exploration [8].

Use of nanoparticle as a promising adsorbent for dye containing effluent remediation is explored [45, 55]. Biogenic nanoparticles have been explored due to its quick

synthesis, faster scaling up, minimal energy requirements and cost effectiveness [50, 55]. Green nanoparticles have proved its competence to degrade highly toxic dyes in simple aqueous mediums [41]. For instance carbon dot-adorned silver nanoparticles synthesized using *Terminalia chebula* fruit extract have been exploited for photocatalytic degradation of methylene blue up to 99.5% and methyl orange upto 99% respectively [44]. Dye remediation by nanoparticles follow either adsorption [54–56] or adsorption with degradation approach [7]. The mechanism of dye degradation by green synthesized nanoparticles starts with the adsorption of dye and is followed by the excitation of nanoparticles by the energy absorption from sunlight that is greater than the band gap energy necessary for electron transfer from the valence band to the particle's conduction band (X. [27, 28]). This step would further lead to creation of holes in the valence band. The electrons are then involved in redox reaction of oxygen (O₂) and water (H₂O) to produce reactive oxygen species like hydroxyl (OH[•]) and superoxide (O₂^{•-}) radicals which are known to attack the complex recalcitrant dye molecule thereby reducing it to simpler products [66]. Silver functionalized magnesium ferrite nanoparticles were capable of removing 95% of malachite green at a rate k of 0.091/min [16]. Similarly, biogenic iron doped Al₂O₃ showed maximum adsorption efficiency of 96.67% with 60 min of reaction [52].

In the present study, green silver nanoflowers were synthesized using *Pongamia pinnata seed cake* (an underutilized by-product from biodiesel industry) and utilized for adsorptive degradation of malachite green (cationic dye). The impact of various parameters on the adsorptive degradation of malachite green by silver nanoflowers (PSCAgNPs) was investigated by one factor at a time (OFAT) approach in order to provide better surface properties to the nanoflower so that it could be effectively explored for the concerned application. Though they are hardly few papers which focus on optimization and its positive impact on enhanced removal capabilities. Moreover the paper also focuses on the Adsorption kinetics, isotherms and the proposes the pathway of malachite green adsorptive degradation by PSCAgNPs.

Materials and methods

Plants and chemicals

Pongamia pinnata seed cake (PSC) was collected from Bioenergy Research, Information and Demonstration Centre (BRIDC), NMAM Institute of Technology, Nitte (13.1859° N, 74.9395° E) campus. Seed cake was fine powdered using blender and used in appropriate proportions for aqueous extract preparation using double distilled water (10 g in 100ml). Silver Nitrate (99%) was

bought from Loba chemie (M/s Loba chemie, Mumbai, India). All other reagents used for the experimentations were of analytical grade unless otherwise mentioned.

Synthesis of PSCAgNPs

10% (w/v) PSC extract was prepared with deionized water. The extract were maintained in an 80 °C water bath for 30 min, after which the water was filtered, and the filtrate was kept at 4 °C for further usage [37]. PSC extract (2.5 mL) was mixed thoroughly with 22.5 mL of 1.0 mM aqueous silver nitrate solution was prepared in deionized water and incubated at room temperature in a shaker (100 rpm). The green synthesis of silver nanoparticle was then confirmed by measuring the absorbance from 360 to 700 nm using a UV–visible spectrophotometer at fixed intervals to detect the colour change along with concentration information (Thermo-Merck, Germany).

Characterization of PSCAgNPs

Once the nanoparticles were successfully biosynthesized using *Pongamia pinnata seed cake powder* extract, they were characterized by various techniques such as FESEM, EDS, particle size and zeta sizer, FTIR and XRD and BET analysis. While EDS focuses on the composition and purity details, FESEM (Carl Zeiss, UK) aids in the analysis of size and shape details. While EDS focuses on the composition and purity details, FESEM (Carl Zeiss, UK) aids in the analysis of size and shape details. Information on the hydrodynamic diameter of the particles in the colloidal solution and the stability features is provided by particle size and zeta-sizer. The plant phytochemicals capped on the nanoflower surface of PSCAgNPs are revealed by FTIR analysis performed by Bruker Alpha (Shimadzu, Japan) and XRD performed by Rigaku Miniflex 600 (Japan), reveals the crystallinity data of the synthesized nanoflowers. Since the PSCAgNPs photocatalytic activity greatly rely on their surface area and total pore volume, BET analysis (Smart Instruments, Mumbai) was conducted to identify these parameters.

Effect of factors on Malachite green removal by synthesized PSCAgNPs

Various parameters such as malachite green concentration (50–200 mg/L), PSCAgNP dosage (25–150 mg/L), agitation speed (60–120 rpm), temperature (25–40 °C), contact time (0–3 h) were varied in order, as per levels given in (Table S1) using OFAT approach. PSCAgNPs concentration was varied from 50- 200 mg/L and temperature was varied from 25–50 °C for malachite green dye degradation. OFAT approach involves studying the effect of one factor on the synthesis of nanoparticles by varying the factor and fixing all the other factors. When the next factor is varied, the value of the previously fixed

factor is maintained at the level at which the maximum output is achieved and thus the process is continued. The effect of these factors on the dye reduction by PSCAgNPs were studied by measuring the UV- spectrophotometric readings at the dyes absorption maxima and % decolourisation was calculated using the formula as

$$\% \text{ Decolourisation} = \frac{C_t - c_0}{c_t} * 100 \quad (1)$$

where C_0 : Concentration of the dye at time 0, C_t : Concentration of the dye at any time t .

Adsorptive Degradation of malachite green by PSCAgNPs

In order to determine the morphological changes on nanoparticles following dye molecule adsorption, FESEM-EDAX (Carl Zeiss, UK) was employed to confirm the adsorption of malachite green dye on PSCAgNPs post nano-remediation. EDAX was also used to analyze the PSCAgNP surface after remediation for the presence of malachite green components. The biosorption process of methyl green on CPAuNPs was described using linearized equations of the PFO, PSO, and IPD models that explain the biosorption kinetics [32, 36]. Additionally, linearized equations of the Langmuir, Freundlich, and Temkin isotherms were used to describe the biosorption mechanism [51]. In order to analyze the methyl green degradation pathway by CPAuNPs, dye solution prior to nanoparticles treatment and post nanoparticles treatment at intermediate times were subjected to LCMS

analysis using Waters synapt G2 (HRMS) equipment operated under APCI mode and the degradation pathway was elucidated. Approximately 2 – 5 μl of sample was injected using 0.1% formic acid in water and acetonitrile in 1:1 ratio (Mobile phase) and a flow rate of 1 ml/min was maintained. Mass spectrometer was operated in positive mode of ionization with nebulizer pressure of 40psi, dry gas temperature of 350 °C and dry gas flow rate of 10 L/min. Adsorptive degradation pathway was then constructed by identifying the degradation metabolites [63].

Results and discussions

Synthesis of CPAuNPs

Formation of PSCAgNPs was confirmed by periodically recording the UV- visible spectrophotometer readings as well as noticing the visual colour changes. Colour changes from colorless to light brown (Fig. 1a), and distinct surface plasmon resonance (SPR) at 430 nm with absorbance value of 0.624 in 24 h (Fig. 1b) was seen which is attributed to monodispersed size variation in the colloidal nanoparticle solution ([27, 28]). However, in case Multiple SPR peaks/ broad spectrum was seen the probable reason could be formation of multi size nanoparticles which results in polydispersity [33].

Characterization of PSCAgNPs

PSCAgNPs nanoflowers in the size range of 18.82–23.70 nm were formed (Fig. 2a). Morphology of PSCAgNPs at different magnifications is shown in (Fig. S1a-c).

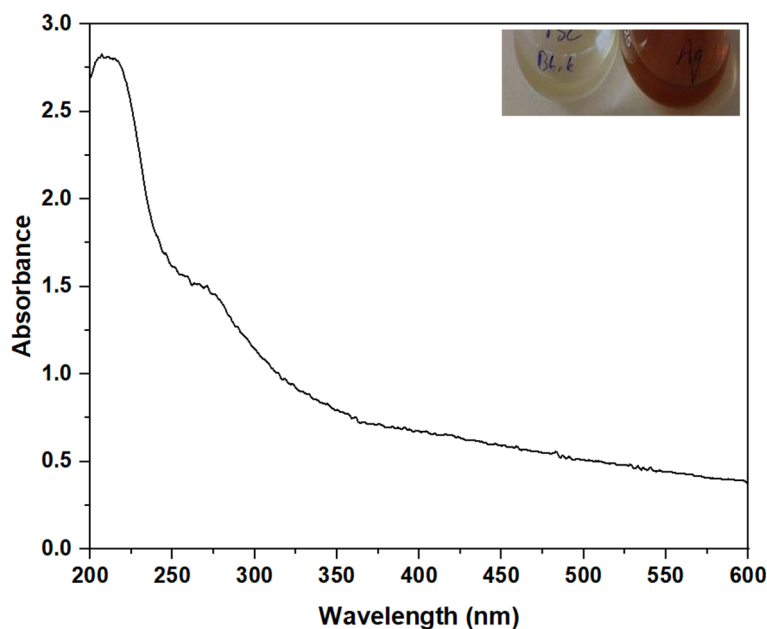


Fig. 1 UV-Vis spectrum of silver nanoflowers synthesised using the seed cake extract of *Pongamia pinnata* (Inset: Visual Observation of colour changes)

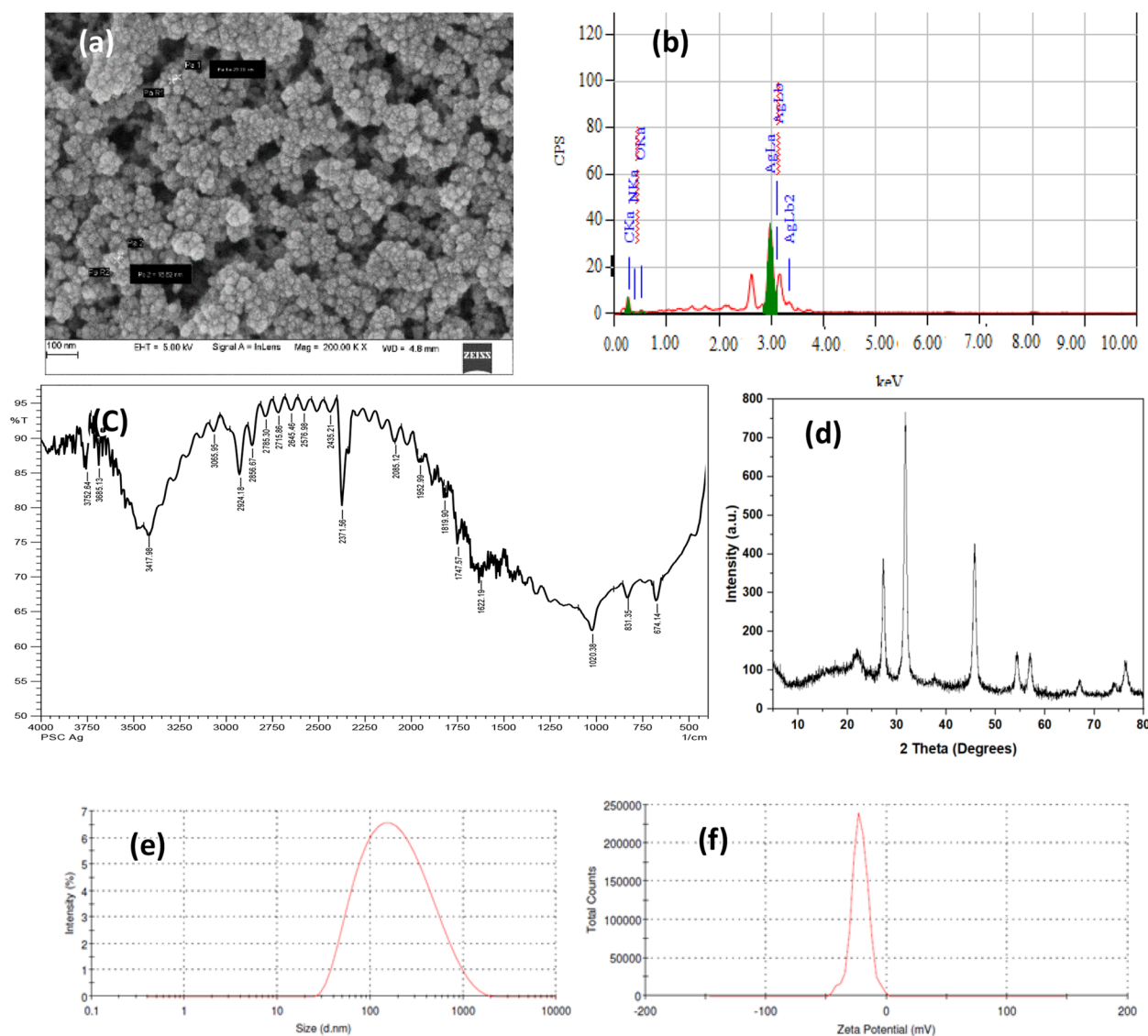


Fig. 2 Characterization of PSCAgNPs by (a) FESEM, (b) EDS, (c) FT-IR, (d) XRD, (e) particle size analysis and (f) zeta potential

Silver nanoparticles synthesized using multiple plant material for extract preparation (*Allium fistulosum*, *Tabernaemontana divaricate* and *Basella alba*) showed size range of nanoparticles of around 50 nm [61]. Green synthesis of silver nanoparticles using *Allium cepa* extract for its antimicrobial potential revealed variety of morphologies which included irregular flowers and spheres [4]. EDS spectrum of PSCAgNPs revealed the weight percent of silver to be 40% (Fig. 2b). The representative peak around 3 keV in EDS spectrum was from the elemental silver [40]. EDS showed some additional C, N and O peaks along with distinctive silver peak which could be from the phytochemicals of PSC capped on the PSCAgNPs surface. C and O peaks were seen in EDS spectrum

of silver nanoparticles biosynthesized from *Chrysanthemum* flower extract [62].

The FTIR peak values of PSCAgNPs indicated the involvement of alcohols and phenolic compounds as reducing agents and proteins as capping biomolecules (Fig. 2c). Probably the presence of proteins and phenolic components seen in the nanoparticles would be due to the seed cake phytochemicals which had successfully capped on the nanoparticle surface (Nayak et al., 2020). FTIR peak at 2924 cm^{-1} corresponds to oligosaccharides and polysaccharides C-H stretching vibration [2], 3752.64 cm^{-1} corresponds to alcohols and phenols O-H stretches as well as amines N-H stretches and 2371 cm^{-1} corresponds to alkanes C-H symmetric and

asymmetric stretching vibrations [48]. Similarly, peak at 3417 cm^{-1} corresponds to OH stretching due to alcoholic group [21], 1622 cm^{-1} corresponds to C=O vibration of –COOH groups for glutamic acid [18]. From the XRD results clear crystalline peaks at 2θ (bragg's angle) of 31.76° , 45.78° and 76.54° corresponded to (1,1,1), (2,0,0) and (3,1,1) planes of silver nanoflowers (Fig. 2d). Availability of seed cake phytochemicals to reduce the metal precursor salt lead to the formation of stable nanoparticle which was crystalline in nature (Rizvi et al., 2022). Additional peaks at 27.28° seen in XRD spectrum may be due to the presence of other biological agents in the seed cake extract. Similarly, XRD results of green silver nanoparticles revealed characteristic peak at 28.3° which was from the biological material [46]. BET analysis showed the maximum surface area and pore volume of PSCAgNPs as $14.79\text{ m}^2/\text{g}$ and 0.0564 cc/g respectively. Biosynthesized silver nanoparticles using goji berry extract as biological substance, were utilized for catalytic degradation of methylene blue (MB) (cationic) and congo red (CR) (anionic) showed surface area of $11.77\text{ m}^2/\text{g}$ with pore volume of 0.027 cc/g during BET evaluation (Kadam et al., 2020). Green synthesized nanoflowers in the present study showed improved surface area values as per BET analysis reports, which could be positively utilised for malachite green dye adsorption and degradation.

PSCAgNPs in the size range of 249.2 nm with 100% intensity, with polydispersity index (PDI) of 0.428, indicated monodispersed nature of the synthesized silver nanoflowers (Fig. 2e). Bigger size of PSCAgNPs when analyzed through particle size analyser in comparison with FESEM accounts to the involvement of capped phytochemicals around the nanoparticles in the size estimation (Hydrodynamic diameter). When morphological results from SEM (50 nm) and particle size analyzer (173 nm) for silver nanoparticles synthesized from *Conocarpus Lancifolius* plant extract were compared, similar results were noticed that could be contributed to denser capping of nanoparticles [39]. The zeta potential was -11.2 mV indicating stable nanoparticles (Fig. 2f). Negative zeta potential values indicates the involvement of negatively charged groups from *Pongamia pinnata* seed cake extract have capped on the surface of PSCAgNPs which gave better dispersity to these nanoflowers [67]. This would further enhance the surface properties of these nanoflowers which could be potentially exploited for the applications [10].

Effect of factors on removal of Malachite green by biogenic PSCAgNP nanoflowers

Effect of dye and PSCAgNP dosage

Malachite green (Aqueous solutions) in the concentration range of ($25\text{--}200\text{ mg/L}$) were incubated with

100 mg/L of PSCAgNP for 3 h @ 30°C and 100 rpm of agitation. It was perceived that the percentage decolourization of malachite green dye increased with increase in dye concentration up to 50 mg/L and later reduced (Fig. 3a). At malachite green concentration of 50 mg/L , nanoparticles dosage of 0.5 g/L and pH of 6, 75% of dye bioremediation was achieved when the temperature of reaction mixture was 35°C [64]. Aqueous solutions of malachite green solutions were incubated with varied concentrations of PSCAgNPs for 3 h at 30°C and 100 rpm which were achieved. It was observed that the percentage decolourization of dye steeply decreased with increase in nanoparticles concentrations of 25 mg/L (Fig. 3b). Thus nanoparticles concentration of 25 mg/L was fixed for PSCAgNPs- MLG combinations (Fig. 3b). Chemically synthesized silver nanoparticles could decolorize malachite green (90%) at pH 7.8, temperature of 30°C and adsorbent dosage $0.1\text{ g}/100\text{ mL}$ [35].

Effect of agitation speed, temperature and time

Aqueous solutions of PSCAgNPs- MG combinations as per optimum conditions from previous experiments were incubated for 3 h at 30°C and varied agitation speeds ($60\text{--}120\text{ rpm}$). It was observed that the percentage decolourization of dye steeply decreased upto 82.25% with increase in agitation speed up to 100 rpm (Fig. 3c). Therefore agitation speed of 60 rpm was fixed for PSCAgNPs- MG combination as it was observed that the percentage decolourization further reduced with increase in agitation speed. Further, aqueous solutions of PSCAgNPs- MG combinations as per optimum conditions from previous experiments were incubated for 3 h and varied temperatures ($25\text{--}40^\circ\text{C}$). It was observed that the percentage decolourization of dye steeply increased upto 86.30% with increase in temperature up to 30°C and later reduced on further increase in temperature (Fig. 3d). Therefore, temperature of 30°C was fixed for further studies. Finally, aqueous solutions of PSCAgNPs- MG combinations as per optimum conditions from previous experiments were incubated for varied time and the dye decolourization percentage was evaluated at intermediate times to find out the maximum decolourization potential. There was a continuous increase in dye decolourization percentage seen with increase in incubation time. The optimum conditions were seen to be 3.5 h for PSCAgNPs- MG combination (Fig. 3e). green synthesized iron nanoparticles from *Acacia nilotica* pod extract were capable of adsorbing 40 ppm of methyl orange in 30 min at 140 RPM with 67.6% dye removal efficiency [14].

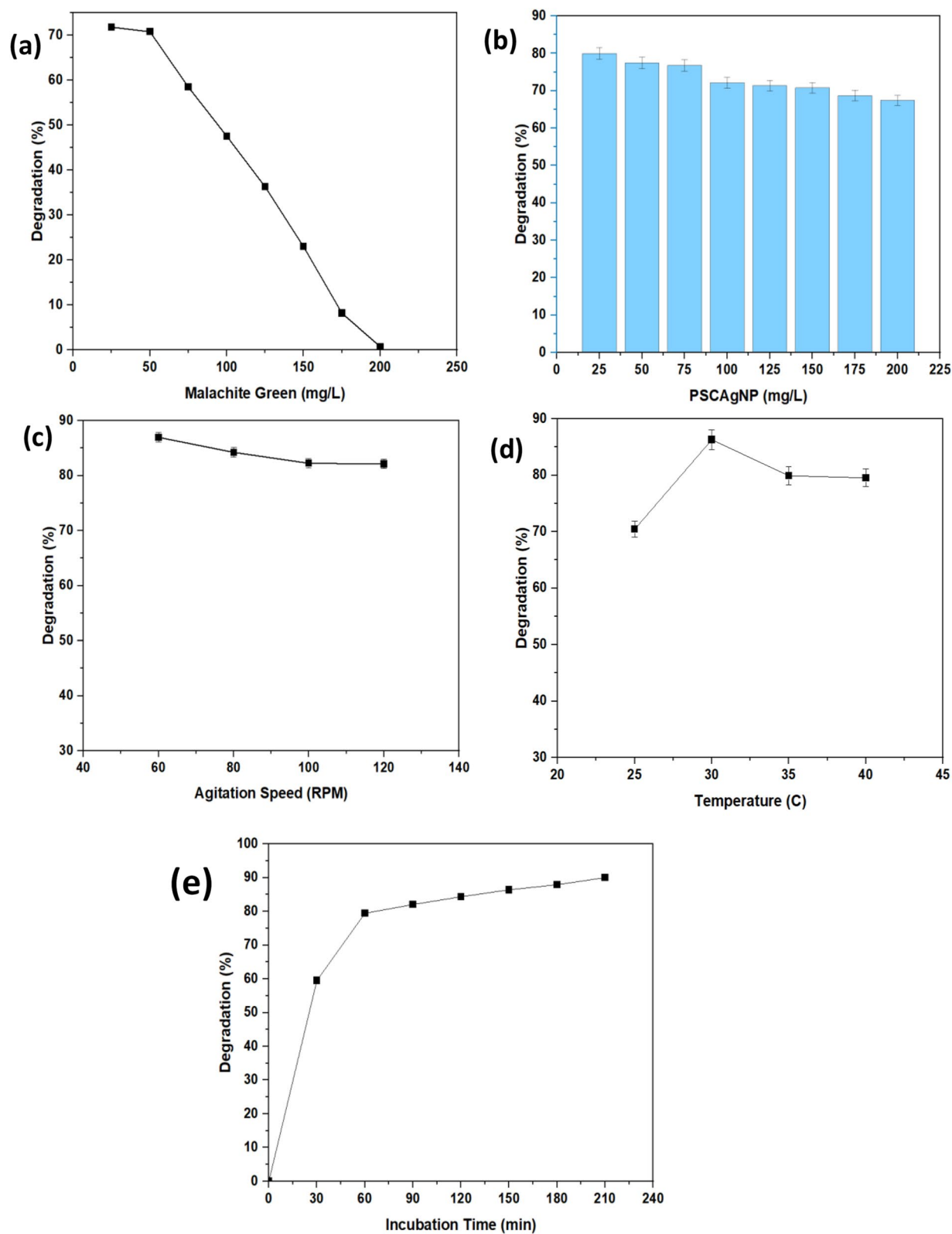


Fig. 3 Effect of variation in Malachite Green (a), PSCAgNPs dosage (b), agitation speed (c), temperature (d) and contact time (e) on Malachite Green removal by PSCAgNPs

Degradation of malachite green dye

FESEM-EDAX analysis confirming adsorption

Biosorption of malachite green on PSCAgNPs was confirmed by FESEM EDAX analysis which confirmed the coating of dye molecules on the surface of the nanoparticles which lead to smoothening of nanoparticles surfaces (Fig S2c) in comparison with FESEM image of PSCAgNPs without methyl green treatment thus confirming the biosorption mechanism (Fig S2a) [26]. The removal of safranin dye using *Bambusa tulda* (biomaterial) led to a similar trend of surface smoothening after treatment [26]. Similar results were seen when TiO₂/Hydrogel nanocomposite was investigated for the removal of brilliant green dye (Aljeboree et al., 2022). The presence of nitrogen was seen in EDAX spectrum of PSCAgNPs- MG (Fig S2d) which was not seen in EDS spectrum of PSCAgNPs (Fig S2b) which confirms the adsorption of Malachite dye (C₅₂H₅₄N₄ O₁₂) on the surface of PSCAgNPs thereby confirming adsorption mechanism. The detailed mechanism of degradation by PSCAgNPs is shown in Fig. 4.

Adsorption kinetics and isotherms

The kinetics model studies for adsorption of MLG by PSCAgNPs using by PFO and PSO models were studied (Fig. 5a and b) [19]. It was evident that the R² values of PSO model was higher compared PFO model (Table 1) and PSO model fitted very well with can be seen with

high R² value of 0.9899 (Table 1). Further Intraparticle diffusion model was plotted to check on the number of rate limiting step by a linear plot of Q_t vs t^{0.5} (Fig. 5c). Although the plot initially exhibited linear behaviour, it did not do so later on. This illustrates that initially the rate is governed by one step and after sometime it depends on multiple reactions (Fig. 5c). IPD studies used for the removal of methyl green by *Cyclea peltata* gold nanospheres showed similar behaviour [36].

In order to determine which model might best portray the results, Langmuir, Freundlich, and Temkin isotherms for the adsorption of MLG on PSCAgNPs were examined. The experimental findings were then fitted into the model equations. Q₀ (mg/g) is the maximum amount of the MLG that is required to form a monolayer on the surface of PSCAgNPs, The plot of specific adsorption (C_e/q_e) versus equilibrium concentration (C_e) (Fig. 6a) revealed that the adsorption followed the Langmuir model, with an R² of 0.994. However the R² values for Freundlich and Temkin isotherms were 0.876 and 0.909 respectively (Fig. 6b and c). This indicates that the adsorption followed unilayer adsorption pattern where good interaction was been between MLG and PSCAgNPs and the reaction was endothermic. Temkin isotherm plot of Methyl orange adsorption by calcinated magnesite showed good linear fit with R²=0.858 which confirmed both dye- dye interaction as well as dye- adsorbent

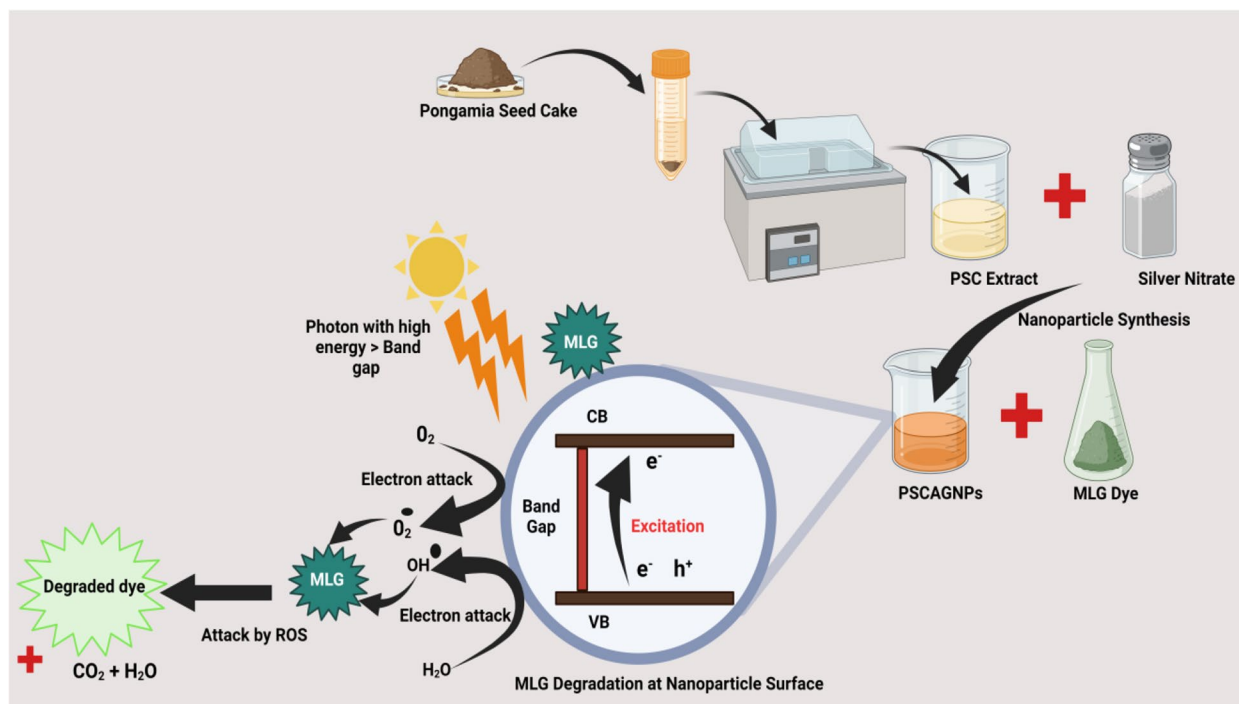


Fig. 4 Mechanism of MLG degradation by PSCAgNP nanoflowers

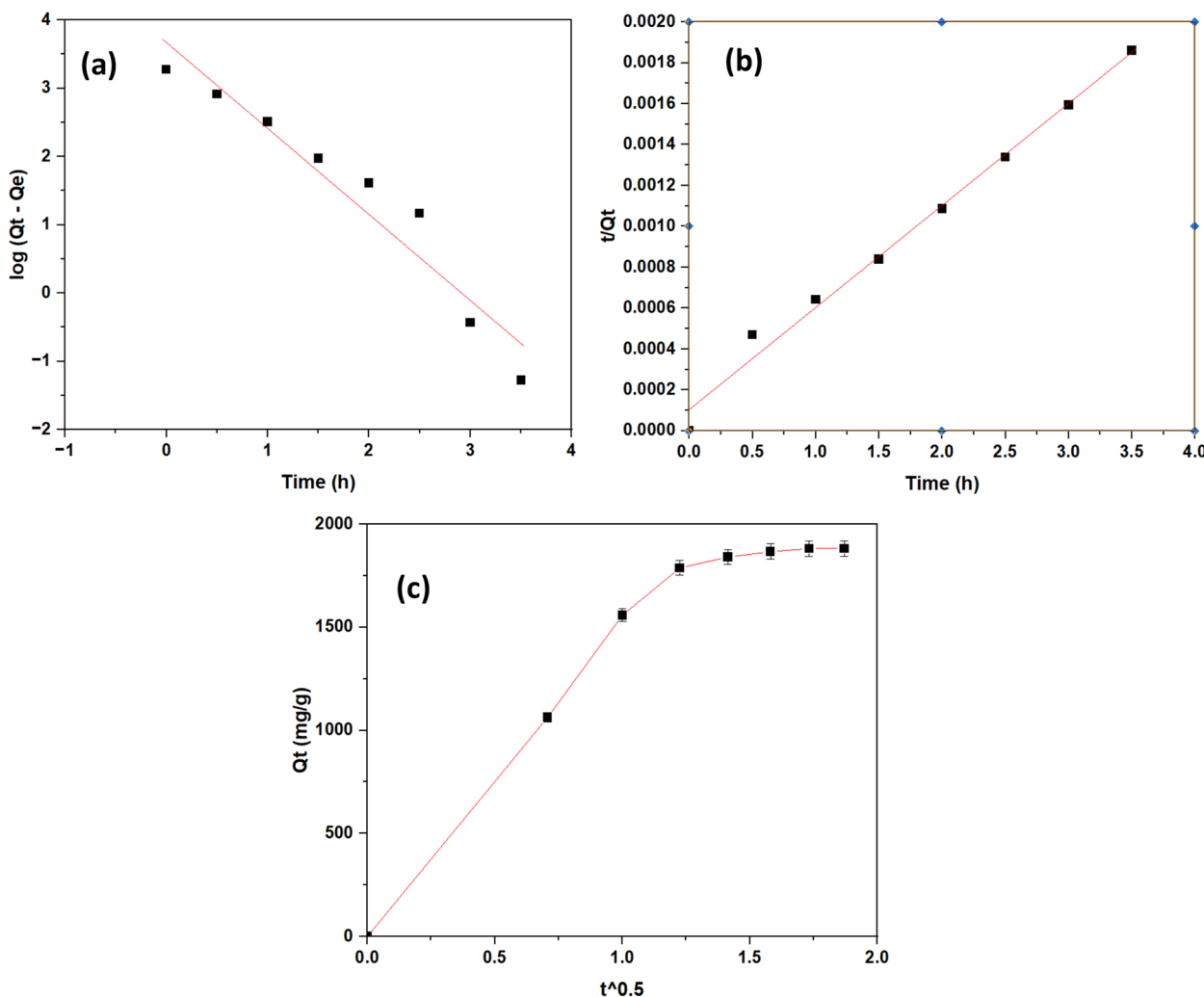


Fig. 5 Kinetic models of Pseudo first order (a) pseudo second order (b) and intraparticle diffusion (c) for adsorption of Malachite Green (50 mg/L) on PSCAgNPs (25 mg/L)

Table 1 Adsorption kinetic parameters of Malachite Green on PSCAgNP

Kinetic Parameters	
Q_e, exp (mg/g)	1881.76
<i>Pseudo-first Order</i>	
k (min^{-1})	2.905
Q_e, cal (mg/g)	3981.072
R^2	0.9307
<i>Pseudo-Second Order</i>	
k^1 (g/mg.h)	2.5E-03
Q_e, cal (mg/g)	2000
R^2	0.9899

interactions control on dye removal process [38]. A comparative table on alternative adsorbent materials used for malachite green removal in comparison with the present study is shown in Table 2.

Degradation pathway of MLG by PSCAgNPs

The intermediates formed upon PSCAgNPs treatment on MLG dye was analyzed by LCMS includes malachite green carbinol (353.13 m/z), aminophenylphenyl methanone (197.94 m/z) dibenzylmethanone (165.01 m/z), dimethyl amino phenyl phenyl methanone (225.38 m/z) and 4-dimethylamino phenol (137 m/z) which undergoes further degradation is shown in supplementary files (Fig S4 and S5) in comparison with the plain MG dye (Fig S3).

Upon interaction of MLG by post optimized PSCAgNPs, within 30 min of incubation hydroxylation of MLG leads to the formation of intermediate product

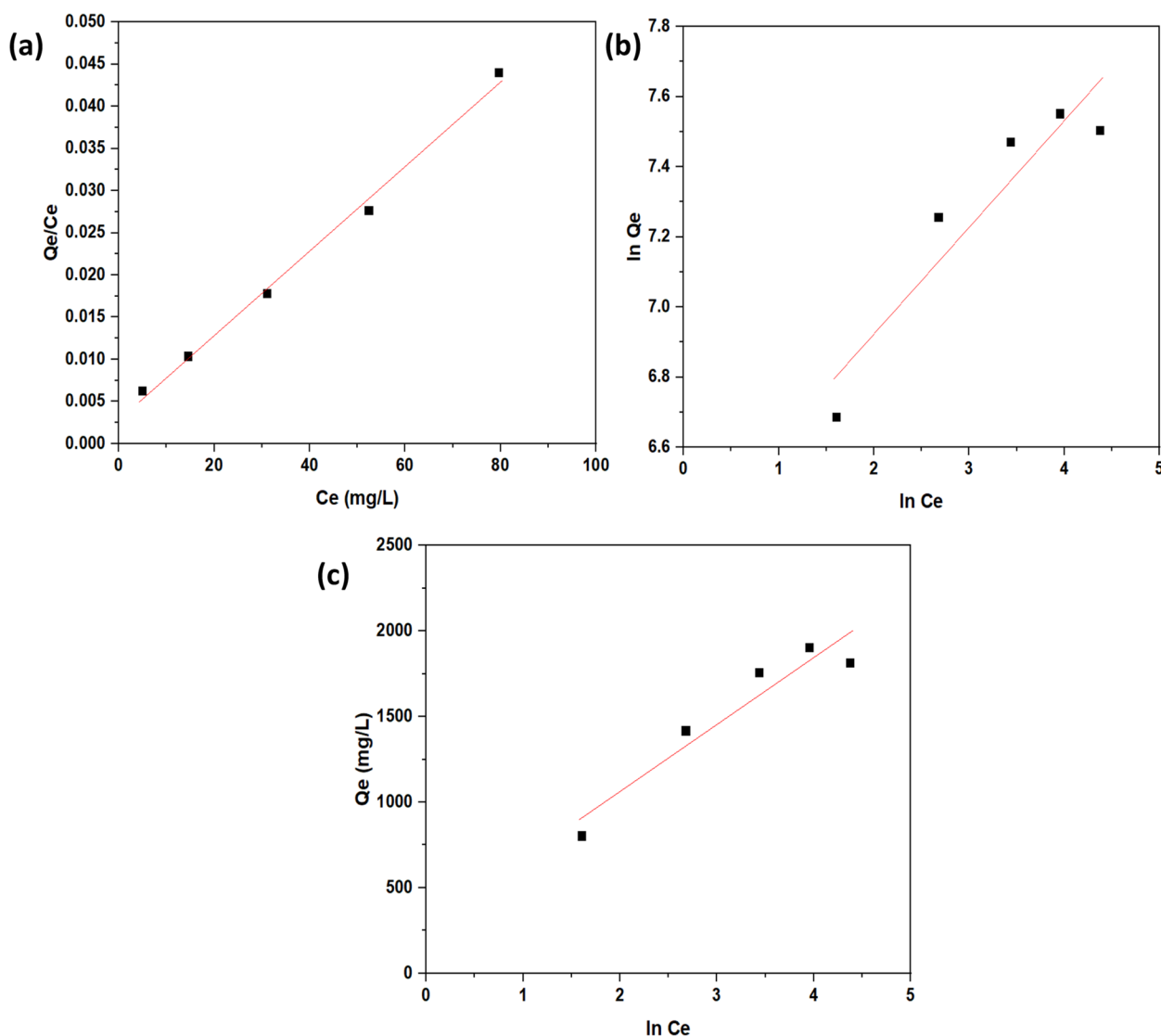


Fig. 6 Adsorption Isotherms of (a) Freundlich, (b) Langmuir (c) and Temkin depicting the equilibrium of MLG adsorption on PSCAgNPs

MLG carbinol which was the first step in the MLG degradation pathway. MLG carbinol further underwent a series of hydroxylation and C–C bond decomposition to form Di – methyl amino phenyl methanone and 4-Dimethyl aminophenol respectively which underwent further degradation which was evident from 60 and 90 min treated LCMS data [15]. Further it was seen that MLG underwent a series of demethylation reaction to form aminophenylphenyl methanone and dibenzylmethanone which is a degraded and less toxic metabolite [11–13]. The proposed degradation pathway for malachite green by PSCAgNPs is shown in Fig. 7. Thus green synthesized PSCAgNPs nanoflowers were

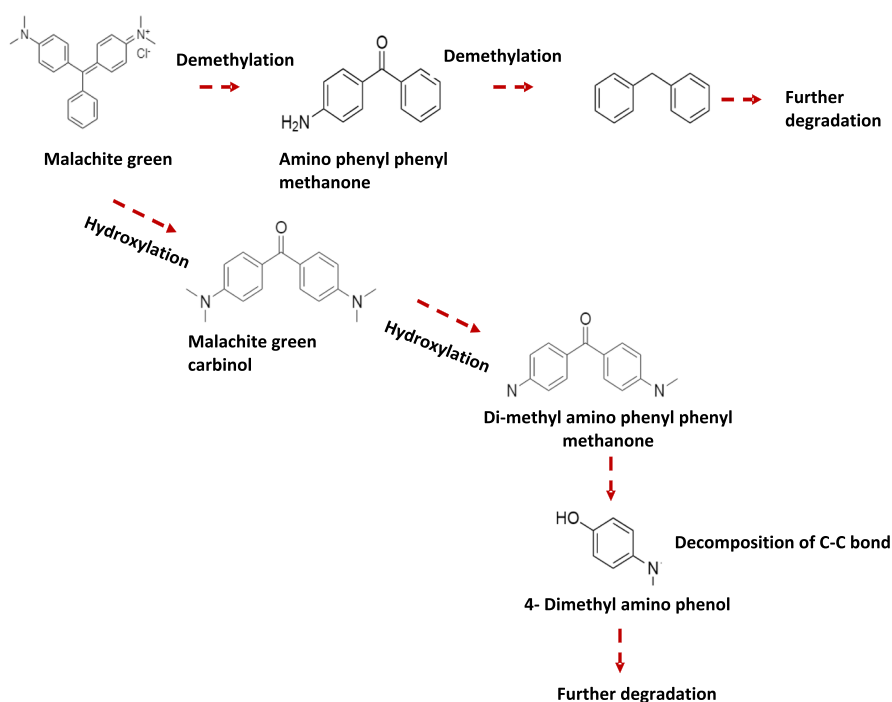
successful in degrading MLG dye to 90% at 50 mg/L of MLG and 25 mg/L of PSCAgNPs dosage.

Cost benefit analysis

Cost of raw material (*Pongamia pinnata* seed cake) used for PSCAgNPs is low; it is also renewable and locally available, this would not only reduce the production cost but even reduce toxic by-product formation. Operational cost would also be low as very less energy is required in comparison with conventional energy intensive physical methods used for nanoparticle production [65]. Other benefits would be the biomaterial itself being nontoxic, and reusable nature of these nanoparticles for multiple

Table 2 Comparative table on alternative adsorbent material used for Malachite green removal

Adsorbent	Adsorbate	Parameters	Adsorption capacity (mg/g)	Percentage removal	Ref
Mn ₃ O ₄ nanoparticles	MLG	Dye conc: 50 mg/L Temp:30 °C Time:20 min Adsorbent dosage: 15 mg	101–162	88.9–92	[60]
Zn(OH) ₂ -AC composite	MLG	Dye conc: 25 mg/L Temp:45 °C Time: 60 min Adsorbent dosage: 0.1 g/100 ml	303.03	96.9	[6]
ZnO Nanoparticles	MLG	Dye conc:50 mg/L Temp:25 °C pH:7 Adsorbent dosage: 0.4 g/L	766.52	99	[31]
(TiO ₂) nanoparticles into H ₂ O ₂ -modified anthracite	MLG	Dye conc:100–400 mg/L Temp:55 °C pH:8 Adsorbent dosage: 0.025 g	320.03	96.2	[47]
Chemically synthesized AgNPs	MLG	Temp:30 °C pH:7.8 Adsorbent dosage: 0.1 g/100 mL	64.51	90	[35]
PSCAgNPs	MLG	Dye conc: 50 mg/L Temp:30 °C Time: 3.5 h Adsorbent dosage: 25 mg/L Agitation Speed: 60 RPM	2000	90.01	Present study

**Fig. 7** Proposed degradation pathway of malachite green by PSCAgNP nanoflowers

cycles [25]. Moreover, enhanced performance of PSCAg-NPs (higher adsorption capabilities) will help in effective removal of dye in wastewater. No doubt, reduced environmental footprint in production, waste reduction, nanoparticle recovery and reuse for multiple cycles, and low carbon footprint during production aligns to the circular economy principles [65]. Unquestionably, this approach definitely strengthens the case for adopting

green nanotechnology in real-world environmental remediation applications, thus ensuring cost efficiency and sustainability.

Conclusions

A unique nano-adsorbent i.e., PSCAgNPs were synthesized using underutilized/ byproduct from biodiesel centre (*Pongamia pinnata* seed cake). The synthesized

nanoflowers were crystalline, of 18.82–23.70 nm size and capped by water soluble phytochemicals of *Pongamia pinnata* seed cake. PSCAgNPs could effectively adsorb residual concentration of MLG ($90.01 \pm 0.17\%$) at 50 mg/L of MLG and 25 mg/L of PSCAgNPs dosage owing to their excellent surface area and outstanding adsorption capabilities. This paper proposes a novel, environmentally responsible and secure remediation method that might be efficiently explored for adsorptive degradation of wastewater containing malachite green. Therefore, green synthesized nanoparticles present a promising avenue for sustainable environmental remediation applications. However overcoming current challenges with respect to stability, toxicity and regulatory hurdles will require more interdisciplinary collaborations, innovations in nanotechnology, and rigorous testing to ensure both effectiveness and environmental safety. With continued research and development in the field, these eco-friendly nanoparticles can revolutionize how we tackle environmental pollution.

Supplementary Information

The online version contains supplementary material available at <https://doi.org/10.1186/s44316-024-00017-8>.

Supplementary Material 1: Fig. S1. FESEM and different magnifications (a) 1 μm , (b) 200nm and (c) 100nm. Fig. S2. (a) FESEM and (b) EDS of synthesized PSCAgNPs pre-treatment and (c-d) post treatment with MLG, confirming adsorptive degradation mechanism. Fig. S3. Mass spectrums of the malachite green dye identified by LCMS (a) Negative ion mode. Fig. S4. Mass spectrums of the malachite green intermediate products identified by LCMS post PSCAgNPs treatment (A) malachite green carbinol (353.13m/z), (B) aminophenylphenyl methanone (197.94 m/z), (C) dibenzylmethanone (165.01 m/z). Fig. S5. Mass spectrums of the malachite green intermediate products identified by LCMS post PSCAgNPs treatment (D) dimethyl amino phenyl phenyl methanone (225.38 m/z) and (E) 4- dimethylamino phenol (137 m/z). Table S1: Levels of factors used in OFAT.

Acknowledgements

The authors acknowledge the support received from NMAMIT, Nitte and Manipal college of Pharmaceutical Sciences Manipal for carrying out this research work. The authors would like to thank Biorender.com for providing icons for creating graphical abstract.

Authors' contributions

S.N wrote the whole manuscript, and LCG prepared a few figures. SPS supervised the work. All authors reviewed the manuscript.

Funding

The study did not receive any funding.

Data availability

No datasets were generated or analysed during the current study.

Declarations

Competing interests

The authors declare no competing interests.

Author details

¹Department of Biotechnology Engineering, NITTE (Deemed-to-Be) University, NMAM Institute of Technology-Affiliated to Nitte, Karkala, Karnataka 574110, India.

Received: 19 August 2024 Accepted: 11 October 2024

Published online: 19 November 2024

References

- Adam MR, Othman MHD, Kurniawan TA, Puteh MH, Ismail AF, Khongnakhorn W, Rahman MA, Jaafar J. Advances in adsorptive membrane technology for water treatment and resource recovery applications: A critical review. *J Environ Chem Eng.* 2022;10: 107633. <https://doi.org/10.1016/j.jece.2022.107633>.
- Ahmadi E, Rezadoost H, Moridi Farimani M. Isolation, characterization, and antioxidant activity of neutral carbohydrates from *Astragalus arbusculinus* gum. *South African J Bot.* 2022;146:669–75. <https://doi.org/10.1016/j.sajb.2021.12.006>.
- Al-Tohamy R, Ali SS, Li F, Okasha KM, Mahmoud YAG, Elsamahy T, Jiao H, Fu Y, Sun J. A critical review on the treatment of dye-containing wastewater: Ecotoxicological and health concerns of textile dyes and possible remediation approaches for environmental safety. *Ecotoxicol Environ Saf.* 2022;231: 113160. <https://doi.org/10.1016/j.jecoen.2021.113160>.
- Ali A, Nazir M, Abbas NA. Green synthesis of silver nanoparticles using *Allium cepa* extract and their antimicrobial activity evaluation. *Chem Int.* 2022;89–94:89. <https://doi.org/10.5281/zenodo.6862470>.
- Althuri A, Tiwari ON, Gowda VTK, Moyong M, Venkata Mohan S. Small/medium scale textile processing industries: case study, sustainable interventions and remediation. *Ind Chem Eng.* 2022;64(1):92–110. <https://doi.org/10.1080/00194506.2020.1821795>.
- Altıntig E, Yenigun M, Sari A, Altundag H, Tuzen M, Saleh TA. Facile synthesis of zinc oxide nanoparticles loaded activated carbon as an eco-friendly adsorbent for ultra-removal of malachite green from water. *Environ Technol Innov.* 2021;21: 101305. <https://doi.org/10.1016/j.eti.2020.101305>.
- Ariaeenejad S, Motamedi E, Salekdeh GH. Highly efficient removal of dyes from wastewater using nanocellulose from quinoa husk as a carrier for immobilization of laccase. *Bioresour Technol.* 2022;349: 126833. <https://doi.org/10.1016/j.biortech.2022.126833>.
- Bayineni VK. Bioremediation of toxic dyes for zero waste. *Biotechnol Zero Waste.* 2022;47–66:47. <https://doi.org/10.1002/9783527832064.ch4>.
- Burkinshaw SM, Salihu G. The role of auxiliaries in the immersion dyeing of textile fibres: Part 1 an overview. *Dye Pigment.* 2019;161:519–30. <https://doi.org/10.1016/j.dyepig.2017.08.016>.
- Chakraborty A, Samriti R, Gupta RK, Cho J, Prakash J. TiO₂ nanoflower photocatalysts: Synthesis, modifications and applications in wastewater treatment for removal of emerging organic pollutants. *Environ Res.* 2022;212:113550. <https://doi.org/10.1016/j.envres.2022.113550>.
- Chaturvedi V, Verma P. Biodegradation of malachite green by a novel copper-tolerant *Ochrobactrum pseudogriponense* strain GGUPV1 isolated from copper mine waste water. *Bioresour Bioprocess.* 2015;2:1–9. <https://doi.org/10.1186/s40643-015-0070-8>.
- Chen CH, Chang CF, Liu SM. Partial degradation mechanisms of malachite green and methyl violet B by *Shewanella decolorationis* NT0U1 under anaerobic conditions. *J Hazard Mater.* 2010;177:281–9. <https://doi.org/10.1016/j.jhazmat.2009.12.030>.
- Chen CY, Kuo JT, Cheng CY, Huang YT, Ho IH, Chung YC. Biological decolorization of dye solution containing malachite green by *Pandora pulmonicola* YC32 using a batch and continuous system. *J Hazard Mater.* 2009;172:1439–45. <https://doi.org/10.1016/j.jhazmat.2009.08.009>.
- Da'na E, Taha A, Afkar E. Green synthesis of iron nanoparticles by acacia nilotica pods extract and its catalytic, adsorption, and antibacterial activities. *Appl Sci.* 2018;8:1922. <https://doi.org/10.3390/APP8101922>.
- Du LN, Wang S, Li G, Wang B, Jia XM, Zhao YH, Chen YL. Biodegradation of malachite green by *Pseudomonas* sp. strain DY1 under aerobic condition: Characteristics, degradation products, enzyme analysis and phytotoxicity. *Ecotoxicology.* 2011;20:438–46. <https://doi.org/10.1007/s10646-011-0595-3>.
- Fernandes RJ, Cardoso BD, Rodrigues AR, Pires A, Pereira AM, Araújo JP, Pereira L, Coutinho PJ. Zinc/magnesium ferrite nanoparticles

- functionalized with silver for optimized photocatalytic removal of malachite green. *Mater*. 2024;17:3158. <https://doi.org/10.3390/MA17133158>.
17. Gowda SAM, Goveas LC, Dakshayini K. Adsorption of methylene blue by silver nanoparticles synthesized from Urena lobata leaf extract: Kinetics and equilibrium analysis. *Mater Chem Phys*. 2022;288: 126431. <https://doi.org/10.1016/J.MATCHEMPHYS.2022.126431>.
 18. Hosseinkhah M, Ghasemian R, Shokrollahi F, Mojdehi SR, Noveiri MJS, Hedayati M, Rezaei M, Salehzadeh A. Cytotoxic potential of nickel oxide nanoparticles functionalized with glutamic acid and conjugated with thiosemicarbazide (NiO@Glu/TSC) against human gastric cancer cells. *J Clust Sci*. 2022;33:2045–53. <https://doi.org/10.1007/S10876-021-02124-2/FIGURES/9>.
 19. Hu Q, Pang S, Wang D. In-depth Insights into mathematical characteristics, selection criteria and common mistakes of adsorption kinetic models: a critical review. *Sep Purif Rev*. 2022;51(3):281–99. <https://doi.org/10.1080/15422119.2021.1922444>.
 20. Ihaddaden S, Aberkane D, Boukerroui A, Robert D. Removal of methylene blue (basic dye) by coagulation-flocculation with biomaterials (bentonite and *Opuntia ficus indica*). *J Water Process Eng*. 2022;49: 102952. <https://doi.org/10.1016/J.JWPE.2022.102952>.
 21. Karthik L, Kumar G, Kirthi AV, Rahuman AA, Bhaskara Rao KV. Streptomyces sp. LK3 mediated synthesis of silver nanoparticles and its biomedical application. *Bioprocess Biosyst Eng*. 2014;37:261–7. <https://doi.org/10.1007/S00449-013-0994-3/TABLES/1>.
 22. Khan A, Roy A, Bhasin S, Emran TB, Khusro A, Eftekhari A, Moradi O, Rokni H, Karimi F. Nanomaterials: An alternative source for biodegradation of toxic dyes. *Food Chem Toxicol*. 2022;164: 112996. <https://doi.org/10.1016/J.FCT.2022.112996>.
 23. Kheradmand A, Negarestani M, Kazemi S, Shayesteh H, Javanshir S, Ghiasinejad H. Adsorption behavior of rhamnolipid modified magnetic Co/Al layered double hydroxide for the removal of cationic and anionic dyes. *Sci Reports*. 2022;12(1):1–17. <https://doi.org/10.1038/s41598-022-19056-0>.
 24. Lahiri SK, Zhang C, Sillanpää M, Liu L. Nanoporous NiO@SiO₂ photocatalyst prepared by ion-exchange method for fast elimination of reactive dyes from wastewater. *Mater Today Chem*. 2022;23: 100677. <https://doi.org/10.1016/J.MTChem.2021.100677>.
 25. Larrañaga-Tapia M, Betancourt-Tovar B, Videira M, Antunes-Ricardo M, Cholula-Díaz JL. Green synthesis trends and potential applications of bimetallic nanoparticles towards the sustainable development goals 2030. *Nanoscale Adv*. 2023;6:51–71. <https://doi.org/10.1039/D3NA00761H>.
 26. Laskar N, Kumar U. SEM, FTIR and EDAX Studies for the removal of Safranin dye from water bodies using modified biomaterial - Bambusa tulda. *IOP Conf Ser Mater Sci Eng*. 2017;225:1–8. <https://doi.org/10.1088/1757-899x/225/1/012105>.
 27. Li T, Jiang W, Liu Y, Jia R, Shi L, Huang L. Localized surface plasmon resonance induced assembly of bimetal nanochains. *J Colloid Interface Sci*. 2022;607:1888–97. <https://doi.org/10.1016/J.JCIS.2021.10.001>.
 28. Li X, Peng Y, Tian T, Wang D, Ren X, Pu X. Nano-flower like NiO modified BiOBr composites with direct Z-scheme: Improved visible light degradation activity for dyes. *J Solid State Chem*. 2022;306: 122715. <https://doi.org/10.1016/J.JSSC.2021.122715>.
 29. Liu X, Chen Z, Du W, Liu P, Zhang L, Shi F. Treatment of wastewater containing methyl orange dye by fluidized three dimensional electrochemical oxidation process integrated with chemical oxidation and adsorption. *J Environ Manage*. 2022;311: 114775. <https://doi.org/10.1016/J.JENVMAN.2022.114775>.
 30. Mani S, Chowdhary P, Bharagava RN. Textile wastewater dyes: toxicity profile and treatment approaches. In: *Emerging and eco-friendly approaches for waste management*. 2018. p. 219–244. https://doi.org/10.1007/978-981-10-8669-4_11.
 31. Mittal H, Morajkar PP, Al Alili A, Alhassan SM. In-situ synthesis of zno nanoparticles using gum arabic based hydrogels as a self-template for effective malachite green dye adsorption. *J Polym Environ*. 2020;28:1637–53. <https://doi.org/10.1007/S10924-020-01713-Y/SCHEMES/2>.
 32. Mona S, Kaushik A, Kaushik CP. Biosorption of reactive dye by waste biomass of *Nostoc linckia*. *Ecol Eng*. 2011;37:1589–94. <https://doi.org/10.1016/J.ECOLENG.2011.04.005>.
 33. Moorthy K, Chang KC, Yu PJ, Wu WJ, Liao MY, Huang HC, Chien HC, Chiang CK. Synergistic actions of phytonutrient capped nanosilver as a novel broad-spectrum antimicrobial agent: unveiling the antibacterial effectiveness and bactericidal mechanism. *New J Chem*. 2022;46:15301–12. <https://doi.org/10.1039/D2NJ02469A>.
 34. Mukherjee A, Goswami N, Dhak D. Photocatalytic remediation of industrial dye waste streams using biochar and metal-biochar hybrids: a critical review. *Chem Africa*. 2022;2022(1):1–20. <https://doi.org/10.1007/S42250-022-00467-5>.
 35. Muthu A, Pandian K, Karthikeyan C, Rajasimman M. Isotherm and kinetic studies on adsorption of malachite green using chemically synthesized silver nanoparticles. *Nanotechnol Environ Eng*. 2017;2:1–17. <https://doi.org/10.1007/s41204-016-0013-4>.
 36. Nayak S, Goveas LC, Selvaraj R, Mutalik S, Sajankila SP. Use of *Cyclea peltata* mediated gold nanospheres for adsorptive degradation of methyl green dye. *Bioresour Technol Reports*. 2022;20: 101261. <https://doi.org/10.1016/J.BITEB.2022.101261>.
 37. Nayak S, Rao CV, Mutalik S. Exploring bimetallic Au–Ag core shell nanoparticles reduced using leaf extract of *Ocimum tenuiflorum* as a potential antibacterial and nanocatalytic agent. *Chem Pap*. 2022;76(10):6487–97. <https://doi.org/10.1007/S11696-022-02299-6>.
 38. Ngulube T, Gumbo JR, Masindi V, Maity A. Calcined magnesite as an adsorbent for cationic and anionic dyes: characterization, adsorption parameters, isotherms and kinetics study. *Heliyon*. 2018;4:1–31. <https://doi.org/10.1016/j.heliyon.2018.e00838>.
 39. Oves M, Ahmar Rauf M, Aslam M, Qari HA, Sonbol H, Ahmad I, Sarwar Zaman G, Saeed M. Green synthesis of silver nanoparticles by *Conocarpus lancifolius* plant extract and their antimicrobial and anticancer activities. *Saudi J Biol Sci*. 2022;29:460–71. <https://doi.org/10.1016/J.SJBS.2021.09.007>.
 40. Padmavathi J, Mani M, Gokulakumar B, Ramesh A, Anantharaj A, Kaviyarasu K. A study on the antibacterial activity of silver nanoparticles derived from *Corchorus aestuans* leaves and their characterization. *Chem Phys Lett*. 2022;805: 139952. <https://doi.org/10.1016/J.CPLETT.2022.139952>.
 41. Parmar M, Sanyal M. Extensive study on plant mediated green synthesis of metal nanoparticles and their application for degradation of cationic and anionic dyes. *Environ Nanotechnology, Monit Manag*. 2022;17: 100624. <https://doi.org/10.1016/J.ENMM.2021.100624>.
 42. Patra AK, Pariti SRK. Restricted substances for textiles. *Text Prog*. 2022;54(1):1–101. <https://doi.org/10.1080/00405167.2022.2101302>.
 43. Peramune D, Manatunga DC, Dassanayake RS, Premalal V, Liyanage RN, Gunathilake C, Abidi N. Recent advances in biopolymer-based advanced oxidation processes for dye removal applications: A review. *Environ Res*. 2022;215: 114242. <https://doi.org/10.1016/J.ENVRES.2022.114242>.
 44. Perumal S, Edison TNJI, Atchudan R, Sundramoorthy AK, Lee YR. Green-routed carbon dot-adorned silver nanoparticles for the catalytic degradation of organic dyes. *Catalysts*. 2022;12:937. <https://doi.org/10.3390/CATAL12090937/S1>.
 45. Rai A, Sirotiya V, Mourya M, Khan MJ, Ahirwar A, Sharma AK, Kawatra R, Marchand J, Schoefs B, Varjani S, Vinayak V. Sustainable treatment of dye wastewater by recycling microalgal and diatom biogenic materials: Biorefinery perspectives. *Chemosphere*. 2022;305: 135371. <https://doi.org/10.1016/J.CHEMOSPHERE.2022.135371>.
 46. Rajeshkumar S, Malarkodi C, Vanaja M, Annadurai G. Anticancer and enhanced antimicrobial activity of biosynthesized silver nanoparticles against clinical pathogens. *J Mol Struct*. 2016;1116:165–73. <https://doi.org/10.1016/J.MOLSTRUC.2016.03.044>.
 47. Ramadan HS, Ali RAM, Mobarak M, Badawi M, Selim AQ, Mohamed EA, Bonilla-Petriciolet A, Seliem MK. One-step fabrication of a new outstanding rutile TiO₂ nanoparticles/anthracite adsorbent: Modeling and physicochemical interpretations for malachite green removal. *Chem Eng J*. 2021;426: 131890. <https://doi.org/10.1016/J.CEJ.2021.131890>.
 48. Rizwana H, Alzahrani T, Alwahibi MS, Aljwaie RM, Aldehaish HA, Alsagabi NS, Ramadan R. Phytosynthesis of silver nanoparticles and their potent antifungal activity against phytopathogenic fungi. *Process*. 2022;10:2558. <https://doi.org/10.3390/PR10122558>.
 49. Rojviroon O, Rojviroon T. Photocatalytic process augmented with micro/nano bubble aeration for enhanced degradation of synthetic dyes in wastewater. *Water Resour Ind*. 2022;27: 100169. <https://doi.org/10.1016/J.WRI.2021.100169>.
 50. Saikia M, Das T, Saikia BK. A novel rapid synthesis of highly stable silver nanoparticle/carbon quantum dot nanocomposites derived from

- low-grade coal feedstock. *New J Chem.* 2021;46:309–21. <https://doi.org/10.1039/D1NJ04039A>.
51. Selvaraj R, Prabhu D, Kumar PS, Rangasamy G, Murugesan G, Rajesh M, Goveas LC, Varadavenkatesan T, Samanth A, Balakrishnaraja R, Vinayagam R. Adsorptive removal of tetracycline from aqueous solutions using magnetic Fe₂O₃ / activated carbon prepared from *Cynometra ramiflora* fruit waste. *Chemosphere.* 2023;310: 136892. <https://doi.org/10.1016/j.chemosphere.2022.136892>.
52. Sharma A, Mittal R, Sharma P, Pal K, Mona S. Sustainable approach for adsorptive removal of cationic and anionic dyes by titanium oxide nanoparticles synthesized biogenically using algal extract of *Spirulina*. *Nanotechnology.* 2023;34: 485301. <https://doi.org/10.1088/1361-6528/ACF37E>.
53. Sharma A, Mona S, Sharma P. Nanomaterials for sustainable remediation: efficient removal of Rhodamine B and lead using greenly synthesized novel mesoporous ZnO@CTAB nanocomposite. *Environ Monit Assess.* 2024;196:1–28. <https://doi.org/10.1007/S10661-024-12655-6/METRICS>.
54. Sharma A, Mona S, Sharma P. Greenly synthesised novel microporous ZnO/GO for adsorption of methyl orange and malachite green. *Int J Environ Anal Chem.* 2024. <https://doi.org/10.1080/03067319.2024.2346198>.
55. Sharma A, Pal K, Saini N, Kumar S, Bansal D, Mona S. Remediation of contaminants from wastewater using algal nanoparticles via green chemistry approach: an organized review. *Nanotechnology.* 2023;34: 352001. <https://doi.org/10.1088/1361-6528/ACD45A>.
56. Sutar S, Patil P, Jadhav J. Recent advances in biochar technology for textile dyes wastewater remediation: A review. *Environ Res.* 2022;209: 112841. <https://doi.org/10.1016/j.envres.2022.112841>.
57. Taheri M, Fallah N, Nasernejad B. Which treatment procedure among electrocoagulation, biological, adsorption, and bio-adsorption processes performs best in azo dyes removal? *Water Resour Ind.* 2022;28: 100191. <https://doi.org/10.1016/j.wri.2022.100191>.
58. Tanveer R, Yasar A, Tabinda A, ul B, Ikhlaiq, A., Nissar, H., Nizami, A.S., Comparison of ozonation, Fenton, and photo-Fenton processes for the treatment of textile dye-bath effluents integrated with electrocoagulation. *J Water Process Eng.* 2022;46: 102547. <https://doi.org/10.1016/j.jwpe.2021.102547>.
59. Tiwari A, Joshi M, Salvi N, Gupta D, Gandhi S, Rajpoot K, Tekade RK. Toxicity of pharmaceutical azo dyes. *Pharmacokinetic Toxicokinetic Considerations.* 2022;11:569–603. <https://doi.org/10.1016/B978-0-323-98367-9.00004-4>.
60. Tran TV, Nguyen DTC, Kumar PS, Din ATM, Qazaq AS, Vo DVN. Green synthesis of Mn₃O₄ nanoparticles using *Costus woodsonii* flowers extract for effective removal of malachite green dye. *Environ Res.* 2022;214: 113925. <https://doi.org/10.1016/j.envres.2022.113925>.
61. Vinodhini S, Vithiya BSM, Prasad TAA. Green synthesis of silver nanoparticles by employing the *Allium fistulosum*, *Tabernaemontana divaricate* and *Basella alba* leaf extracts for antimicrobial applications. *J King Saud Univ - Sci.* 2022;34: 101939. <https://doi.org/10.1016/j.jksus.2022.101939>.
62. Wan H, Huang Q, Mia R, Tao X, Mahmud S, Liu H. Bioreduction and stabilization of nanosilver using chrysanthemum phytochemicals for antibacterial and wastewater treatment. *ChemistrySelect.* 2022;7: e202200649. <https://doi.org/10.1002/slct.202200649>.
63. Wang Z, Ren D, Zhang X, Zhang S, Chen W. Adsorption-degradation of malachite green using alkali-modified biochar immobilized laccase under multi-methods. *Adv Powder Technol.* 2022;33: 103821. <https://doi.org/10.1016/j.apt.2022.103821>.
64. Weng X, Huang L, Chen Z, Megharaj M, Naidu R. Synthesis of iron-based nanoparticles by green tea extract and their degradation of malachite. *Ind Crops Prod.* 2013;51:342–7. <https://doi.org/10.1016/j.indcrop.2013.09.024>.
65. Yadav S, Raman APS, Singh MB, Massey I, Singh P, Verma C, Alfantazi A. Green nanoparticles for advanced corrosion protection: Current perspectives and future prospects. *Appl Surf Sci Adv.* 2024;21: 100605. <https://doi.org/10.1016/j.apsadv.2024.100605>.
66. Yadav VK, Gupta N, Kumar P, Dashti MG, Tirth V, Khan SH, Yadav KK, Islam S, Choudhary N, Algahtani A, Bera SP, Kim DH, Jeon BH. Recent advances in synthesis and degradation of lignin and lignin nanoparticles and their emerging applications in nanotechnology. *Materials.* 2022;15:953. <https://doi.org/10.3390/MA15030953>.
67. Zeng N, Zhao H, Liu Y, Wang C, Luo C, Wang W, Ma T. Optimizing of the colloidal dispersity of silica nanoparticle slurries for chemical mechanical polishing. *Silicon.* 2021;14(13):7473–81. <https://doi.org/10.1007/S12633-021-01448-Y>.

Publisher's Note

Springer Nature remains neutral with regard to jurisdictional claims in published maps and institutional affiliations.